Analytical and Bioanalytical Chemistry (2021) 413:555–564
https://doi.org/10.1007/s00216-020-03026-4

RESEARCH PAPER

# Functionalization of hybrid surface microparticles for in vitro cellular antigen classification

Brandon K. Ashley[1] · Jianye Sui[2] · Mehdi Javanmard[1,2] · Umer Hassan[1,2,3]

Received: 11 September 2020 / Revised: 7 October 2020 / Accepted: 23 October 2020 / Published online: 6 November 2020


## Abstract

Hybrid material surfaces on microparticles are emerging as vehicles for many biomedical multiplexing applications. Functionalization of these hybrid surface microparticles to biomolecules presents unique challenges related to optimization of surface chemistries including uniformity, repeatability, and sample sparring. Hybrid interfaces between microlevel surfaces and individual biomolecules will provide different microenvironments impacting the surface functionalization optimization and efficiency. Here, we propose and validate the first demonstration of streptavidin adsorption–based antibody functionalization on unmodified, hybrid surface microparticles for in vitro analysis. We test this analytical technique and fabricate hybrid surface microparticles with a polystyrene core and aluminum oxide semi-coating. Additionally, we optimize the streptavidin-biotin functionalization chemistry in both assay implementation and sample sparring via analytical mass balances for these microparticles and subsequently conjugate anti-human CD11b antibodies. Result confirmation and characterization occurs from ultraviolet protein absorbance and ImageJ processing of fluorescence microscopy images. Additionally, we design and implement the multi-sectional imaging (MSI) approach to support functionalization uniformity on the hybrid surface microparticles. Finally, as a proof-of-concept performance, we validate anti-CD11b antibodies functionalization by visualizing hybrid surface microparticles conjugate to human neutrophils isolated from blood samples collected from potentially septic patients. Our study introduces and defines a category of functionalization for hybrid surface microparticles with the intent of minuscule sample volumes, low cost, and low environmental impact to be used for many cellular or proteomic in vitro multiplexing applications in the future.

**Keywords** Hybrid surface · Surface functionalization · Streptavidin · Multiplexing · Eco-conscious

## Introduction

Microparticles fabricated with hybrid material surfaces have paved the way for a new class of active targeting agents for multiplexing applications in disease treatment and diagnostics [1, 2]. Newer fabrication techniques and technologies have improved hybrid surface microparticles (also known as Janus particles) manufacturing at large scales using a myriad of materials and geometries to facilitate high-throughput delivery [3, 4]. However, challenges arise as employing surface modifications towards micro- and nanoscale particles with different surface materials as they behave to reagents and chemistries differently. A plethora of functionalization methods and mechanisms have been recently published for hybrid surface micro- and nanoparticles, but are developed for specific intentions with unique surface chemistries that cannot translate to other materials or applications [5–9]. To ensure that these hybrid particles are practical and have clinical potential, simple yet universal and effective functionalization protocols must be utilized with different material surfaces demonstrating equal binding strength and immobilization distribution.

Functionalization to hybrid microparticles can be validated by demonstrating their effective conjugation to human blood cells—in particular, leukocyte surface receptors. Leukocytes

**Supplementary Information** The online version contains supplementary material available at https://doi.org/10.1007/s00216-020-03026-4.

✉ Umer Hassan
umer.hassan@rutgers.edu

[1] Department of Biomedical Engineering, Rutgers, The State University of New Jersey, Piscataway, NJ 08854, USA

[2] Department of Electrical Engineering, Rutgers, The State University of New Jersey, Piscataway, NJ 08854, USA

[3] Global Health Institute, Rutgers, The State University of New Jersey, New Brunswick, NJ 08901, USA

play a critical role in activating the acquired immune response and subsequently identifying and eliminating various pathogens with different origins and properties [10]. Numerous cell surface receptor densities and their differential regulation provide insights on cellular activity and pathophysiological signaling. These biomarkers are commonly used for diagnosis and management of many diseases such as sepsis, HIV, and rheumatoid arthritis [11–15]. The clinical standard to quantify these biomarkers includes flow cytometry, which fluorescently stains different surface receptors. Unfortunately, flow cytometry presents many technological challenges including limited multiplexing, necessitates large fluid volumes extracted from patients, and requires trained professionals to operate and interpret results [12, 16–20]. Alternative cellular antigen multiplexing technologies can be developed using hybrid surface microparticles and their effective functionalization to overcome these limitations.

Recently, we have reported the fabrication of hybrid surface microparticles that exhibit unique impedance responses by modulating different metal oxide layer thicknesses semi-coating their surface [21]. These particles can introduce new opportunities for cellular classification techniques, as microparticles fabricated with different metal oxides and thickness can target unique biomarkers, serving as an alternate to flow cytometry for multiplex quantification of cellular antigens. Our hybrid surface microparticles can potentially be used with microfluidic impedance–based sensing technologies and capable of translating to point-of-care diagnostic sensors [22–24]. The proper surface modifications of our metal oxide–coated hybrid surface microparticles are critical for numerous cellular conjugations and similarly multiplexing applications [1].

Here, we develop and characterize an anti-CD11b antibody functionalization protocol on hybrid material particles using a streptavidin-biotin linker to improve point-of-care multiplexing technology. The hybrid surface nature of the particles used consists of a polystyrene core semi-coated with aluminum oxide ($Al_2O_3$) on half of the surface. For analytical purposes, we targeted CD11b receptors predominately expressed on neutrophils. CD11b neutrophils are newly explored sepsis biomarkers, as they participate in the CR3 integrin heterodimer with CD18 and increase adhesion between immune cells to activate a pro-inflammatory response [25, 26]. The biotinylated anti-CD11b antibodies bind with unmodified streptavidin adsorbed to both hybrid surfaces through protein corona kinetics [27, 28]. Protein corona formation around the particles is what drives functionalization rather than hinders it as is the case for many heterogeneous or in vivo biological processes [29]. Streptavidin protein acts as the bi-linker and has a heterotetrametric structure with four active sites for biotin binding on different planes. This ensures that it remains functional during adsorption when the protein undergoes slight structural modifications at the particle surface interface [30]. Additionally, as the streptavidin protein physiologically adsorbs to the hybrid surface particle, its surface interaction should remain independent of aluminum oxide or bare polystyrene surfaces, and result in the uniform functionalization distribution around the particle [31]. Polypropylene tubes and cuvettes are used to mitigate non-specific adsorption to those surfaces, as they are material of choice for inexpensive plastic containers [32]. While previous results have found similar streptavidin adsorption densities for different materials [29, 33, 34], none has yet explored coverage for different materials on the same microparticle. Biotinylated antibodies subsequently attach to the particles through streptavidin-biotin affinity binding consisting of hydrogen bonds and Van der Waals forces [29, 35]. Streptavidin-biotin chemistry is simple as it requires minimal intermediate processing steps and accessory reagents, thus allowing high-throughput processing with minimal cost or time [36–38].

Our work is the first demonstration of a uniform antibody functionalization protocol for multiple material surfaces on the same microparticle using a streptavidin-biotin linker, visualized by Fig. 1. Our conjugation chemistry requires low sample volumes and low-cost materials and results in effective conjugation with uniform coverage around the particle. Furthermore, we provide an analytical method to model adsorption saturation on polystyrene-$Al_2O_3$ hybrid particle surfaces and present a "reagent sparring" protocol based on different particle sizes and concentrations for straightforward translations with other applications. We also design and implement the multi-sectional imaging (MSI) approach to validate the uniformity of functionalization on our hybrid surface microparticles. Finally, we demonstrate successful functionalization by observing treated microparticles passively targeting human neutrophils in vitro. Such protocols and characterizations are detailed in the following sections.

## Materials and methods

### Materials

Lyophilized streptavidin (> 11 U per mg of protein lyophilized in 10 mM phosphate-buffered saline), phosphate-buffered saline (PBS, 1× and 10×, pH = 7.2), dimethyl sulfoxide (DMSO, ≥ 99.9% purity), biotin-4-fluorscein, Ficoll-Paque density gradient, and Roswell Park Memorial Institute medium 1640 (RPMI) were purchased from Sigma-Aldrich (St. Louis, MO, USA). Biotinylated anti-CD11b monoclonal mouse antibody (> 95% purity) and 1.5-mL polypropylene microcentrifuge tubes were purchased from Thermo Fisher Scientific (Waltham, MA, USA). The VWR UV-Vis Spectrophotometer 1200 and UV polypropylene disposable ultra-micro cuvettes were purchased from VWR (Radnor, PA, USA). Unidentifiable human blood was obtained from Robert Wood Johnson Medical Hospital (New Brunswick, NJ, USA) through an institutional review

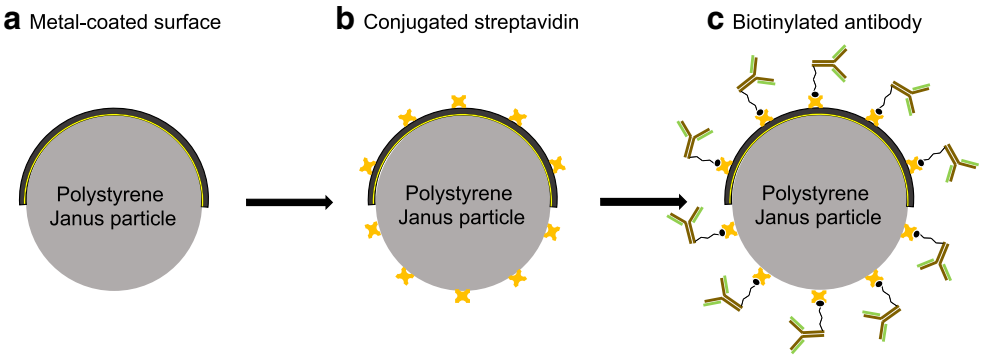


**Fig. 1** Scheme for functionalization and microfabricated hybrid surface particles with one half of the particle coated with gold and aluminum oxide (**a**). Here, streptavidin (yellow x's) adsorbs to the hybrid surface particle uniformly on all materials (**b**). Biotinylated antibodies then bind through the streptavidin conduit (**c**)

board (IRB) study. Type I deionized water was used in all experiments for both sample preparation and washing procedures.

## Hybrid surface microparticle fabrication

Hybrid surface microparticles were fabricated using nanosphere lithography where self-assembly occurs on glass after polystyrene drop-casting, producing 3-μm polystyrene microparticles which are used as the microparticle core. Electron-beam deposition then deposits 20 nm of gold above the exposed half of the particles to act as the adhesive layer for the aluminum oxide. Following this, the aluminum oxide layer is coated through atomic layer deposition. In this step, the thickness can be modulated from 5 to 30 nm to produce particles with unique electrical properties. Electrical differentiation of the particles is possible with a 10 nm difference in the thickness as shown in our earlier study. For our current study, an aluminum oxide layer of 30 nm thickness was utilized [21]. Finally, particles were suspended in 1× PBS through ultrasonic agitation for 30 min. The resulting hybrid surface particle is conceptually represented by Fig. 1a.

## Anti-CD11b antibody surface functionalization to microparticles

Following particle fabrication, streptavidin chemistry is incorporated for particle surface functionalization. To begin, lyophilized streptavidin was reconstituted in 1× PBS, with vortexing for 10 s followed by ultrasonic agitation for 10 min to ensure uniform concentration and dispersion of the streptavidin solution. Once active, 2 μL of streptavidin (0.1 mg/mL) was added into 200 μL of microparticle solution ($5.92 \times 10^7$ particles/mL) and incubated as a mixture for 12 h at 0 °C. The incubation period is critical to allow for the streptavidin corona formation upon the particle surface and ensure high stability binding [29]. Once incubated, the solution was centrifuged for 10 min at 10,000*g* as the mass gradient purifies microparticles from the unattached streptavidin proteins in solution. After supernatant removal, the particle pellet was subjected to further purification steps to reduce unbound streptavidin. This included pellet resuspension in 170 μL of deionized water and 20 μL 1× PBS, 10 min of ultrasonic agitation, and another step of centrifugation at 10,000*g* for 10 min. Reducing free-floating streptavidin is imperative so it does not competitively bind with the biotinylated antibodies to be introduced in subsequent steps. At this stage, particle functionalization is represented by Fig. 1b.

Following streptavidin adsorption to microparticles, biotinylated antibodies were added to enable antibody functionalization. Here, 10 μL of biotinylated anti-CD11b antibody (1 mg/mL in 1× PBS) was combined with the streptavidin-adsorbed microparticle solution (1× PBS) and further incubated for 8 h at 0 °C for biotin-streptavidin binding to reach equilibrium. Similar to streptavidin purification following incubation, the solution was washed with the same conditions and parameters to isolate microparticles and separate out unbound antibodies. A fully functionalized hybrid surface particle is represented by Fig. 1c, with biotinylated antibodies bound to the adsorbed streptavidin.

## Streptavidin loading determination using spectrophotometry

Streptavidin concentration before and after washing was quantified using UV absorbance to indirectly determine streptavidin adsorption loading on the hybrid surface particles [39, 40]. Initially, a standard curve must be developed to identify a relationship of absorbance versus streptavidin concentration. Disposable UV-sensitive ultra-micro cuvettes were loaded with 70 μL of streptavidin samples with concentrations from 0.1 to 2.0 μg/mL. The VWR UV-Vis Spectrophotometer 1200 was used to analyze samples at 280 nm wavelength.

## Biotin-4-fluorescein enabled fluorescence microscopy

Biotin-4-fluorescein (B4F) was dissolved in dimethyl sulfoxide (DMSO) to form a 0.08 mg/mL solution. After streptavidin addition to the microparticle solution, incubation and washing steps were performed prior to adding anti-CD11b antibodies. Subsequently, 10 μL of B4F in DMSO (0.08 mg/mL) was added to a 200 μL sample. This was

followed by 10 s of vortexing and 5 min of ultrasonic agitation to thoroughly mix B4F with the streptavidin-adsorbed microparticles, as DMSO and 1× PBS combine. After mixing, the sample was incubated for 1 h to ensure strong streptavidin-biotin binding before fluorescence analysis.

### ImageJ processing, analysis, and analytical quantification

ImageJ was used for image processing and fluorescent quantification. For particle pixel intensity compared to background pixel intensity, a line segment was aligned connecting particles across the image space and pixel values were recorded from the "Distribution" function under the "Analyze" tab. For recording maximum pixel intensity from particles, rectangular segments were aligned over particle regions and max values were recorded from the "Measure" function under the "Analyze" tab.

### Neutrophil isolation from whole blood

Patient blood samples were collected from Robert Wood Johnson Medical Hospital. Following collection, the blood is processed to isolate human neutrophils. Blood was combined with equal parts 1× PBS, and 1.8 mL was mixed with 2.4 mL of Ficoll-Paque density gradient. The solution was centrifuged for 30 min at 400*g* to separate plasma, platelets, and red blood cells, followed by supernatant aspiration and addition of 3 mL of deionized water for 15 s to lyse non-neutrophil mononuclear cells. After 15 s, 0.3 mL of 10× PBS was added for tonicity restoration, and the solution was further centrifuged for 5 min at 300*g*. The previous step was repeated until a neutrophil pellet is formed, which was resuspended in RPMI 1640 with 50 μL of cells to 5 mL of media. Once prepared, 200 μL solution of anti-CD11b antibody ($5.92 \times 10^7$ particles/mL) functionalized hybrid particles was mixed with 1 mL of cells in RPMI 1640 media followed by 1-h incubation with subsequent imaging. A final scheme for experimental procedures is detailed by Fig. 2.

## Results and discussion

### Determining and characterizing theoretical streptavidin adsorption yields

When evaluating final protein corona kinetics on surfaces with streptavidin, an experimental maximum of $4.4 \times 10^{11} \pm 0.7 \times 10^{11}$ streptavidin molecules per $cm^2$ has been previously concluded [29]. Such coverage comes from the potential electrostatic hindrances for streptavidin at 7.2 pH which is negatively charged in these conditions from its isoelectric point value of 5.0, as well as the adsorbing surface angle of curvature, particle size, surface shape, surface hydrophobicity, and steric hindrance [29, 41–44]. Accounting for streptavidin dimensions, microparticle concentration, particle size, and initial/final solution concentrations after surface loading, we developed an analytical method to optimize experimental conditions and as an estimate for retaining material yields during functionalization protocols while still delivering fully realized targeting agents.

First, the optimal coverage percentage is determined by balancing the total streptavidin surface area ($A_{\text{streptot}}$) to total adsorbing surface area ($A_{\text{JPtot}}$) in a fully saturated solution (Eq. 1).

$$\text{Coverage}\% = \frac{A_{\text{streptot}}}{A_{\text{JPtot}}} \tag{1}$$

This can be further expanded by the total number of streptavidin molecules ($N_{\text{strep}}$) and total number of microparticles in solution ($N_{\text{JPtot}}$) for one streptavidin molecule ($A_{\text{strep}}$) and one microparticle respectively ($A_{\text{JP}}$; Eq. 2):

$$\text{Coverage}\% = \frac{N_{\text{strep}} A_{\text{strep}}}{N_{\text{JP}} A_{\text{JP}}} \tag{2}$$

where $N_{\text{strep}}$ can be expanded by dividing the change in supernatant concentration after removing particles with adsorbed streptavidin ($C_{\text{strep,in}} - C_{\text{strep,out}}$) which is also considered the minimum initial concentration required for all streptavidin to be absorbed as $C_{\text{min}}$ when $C_{\text{strep,out}}$ equals zero by the molecular weight of streptavidin ($Mw_{\text{strep}}$). In addition, $A_{\text{strep}}$ is evaluated as the average surface area for one interacting face of streptavidin, $N_{\text{JP}}$ is extrapolated from the microparticle concentration ($P_{\text{JP}}$), and $A_{\text{JP}}$ is determined by the surface area of a sphere considering half the particle with the polystyrene radius ($R_{\text{PS}}$) and the other half with the deposited gold and $Al_2O_3$ layers ($R_{\text{ox}}$). While volume should be included for $N_{\text{strep}}$ and $N_{\text{JP}}$, the two together cancels each other out:

$$\text{Coverage}\% = \frac{C_{\text{min}} A_{\text{strep}}}{Mw_{\text{strep}} P_{\text{JP}} 2\pi \left(R_{\text{PS}}^2 + R_{\text{ox}}^2\right)} \tag{3}$$

Finally, the maximum streptavidin surface density ($K$) of $4.4 \times 10^{11} \pm 0.7 \times 10^{11}$ molecules per $cm^2$ is factored with the critical concentration change from streptavidin adsorbed to particle surfaces (Eq. 4) and can be substituted into Eq. 3 to determine the theoretical critical coverage (Eq. 5):

$$C_{\text{crit}} = K Mw_{\text{strep}} P_{\text{JP}} 2\pi \left(R_{\text{PS}}^2 + R_{\text{ox}}^2\right) \tag{4}$$

$$\text{Critical Coverage}\% = K A_{\text{strep}} \tag{5}$$

From Eq. 5, critical coverage evaluation is independent of hybrid microparticle concentration or size, solely

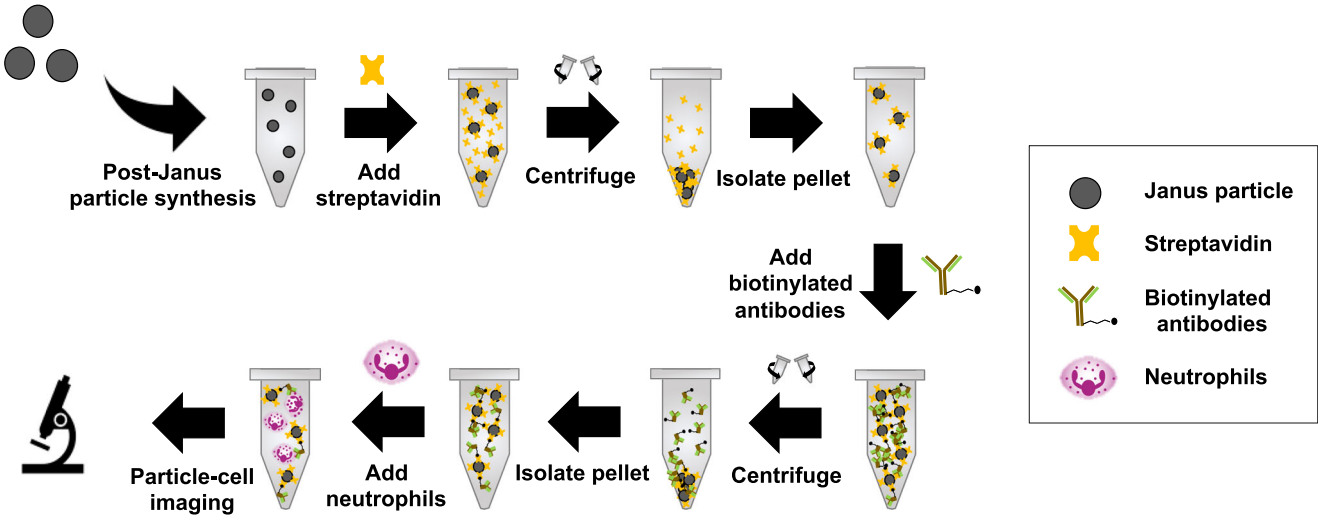


**Fig. 2** Graphical representation of experimental procedures after Janus particle fabrication. Hybrid microparticle is labeled as Janus particle

dependent on the critical surface density for streptavidin and the interacting face for one streptavidin molecule. Using an estimated value of 21 $nm^2$ (given streptavidin molecular dimensions of 4.2 nm × 4.2 nm × 5.5 nm [45]) the maximum coverage percentage for streptavidin is 9.24 ± 1.47% coverage. The trend is linear with respect to initial concentration and is represented by Fig. 3a.

Using initial experimental parameters from this study, it results in a 0.70 ± 0.11 μg/mL minimum streptavidin concentration required for the saturated coverage. These conditions arise from using a 55-kDa weight for streptavidin ($Mw_{strep}$), 21 $nm^2$ for $A_{strep}$, $5.92 \times 10^7$ particles/mL for $P_{JP}$, 1.5 μm for $R_{PS}$, and 1.55 μm for $R_{ox}$ when considering the 20-nm gold and 30-nm $Al_2O_3$ layers. After determining the critical coverage of 9.24 ± 1.47%, Eq. 3 can be used to further determine critical sample yields when variables change. As shown by Fig. 3b, changing the microparticle concentration or particle size affects the streptavidin concentration required for coverage saturation, as derived from Eq. 3. From the trends, streptavidin concentration has a positive linear relationship with Janus particle concentration and has an exponential relationship to increasing particle size:

$$C_{min} \propto P_{JP} C_{min} \propto R_{PS}^2$$

The optimal streptavidin concentration required can be empirically determined for various conditions by the streptavidin relationship with coverage percentage on the particle surfaces from Eq. 3 and can be used as a theoretical reference when validating experimental results.

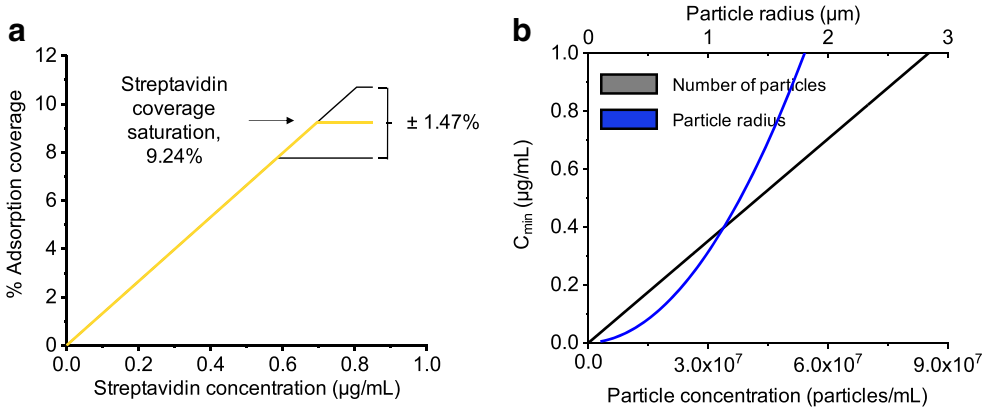


**Fig. 3** Characterizing and optimizing streptavidin adsorption and particle concentration. **a** Modeled relationship between streptavidin concentration (in μg/mL) and % surface area covered by adsorbed streptavidin on particle surfaces considering the study's experimental conditions. Here, streptavidin reaches kinetic adsorption saturation at 9.24 ± 1.47% coverage. Minimum streptavidin concentration ($C_{min}$) for the study's experimental conditions to achieve saturation coverage. **b** A modeled linear relationship between particle concentration (particles/mL) and streptavidin concentration required to achieve saturated adsorption with 1.5 μm particle radius (bottom axis, black line). Exponential relationship between particle radius (μm) and streptavidin concentration for constant particle concentration used during experimentation (top axis, blue line). Relationships assume proper incubation times for long-term adsorption kinetics to apply

## Optical absorbance curve and experimental streptavidin coverage

The UV absorbance curve for given concentrations develops a relationship to confirm unknown sample concentrations (Electronic Supplemental Material (ESM) Fig. S1 and Table S1). The difference between the measured streptavidin concentrations from the initial sample at 0.1 μg/mL and the measured supernatant after the first centrifugation determines the amount of streptavidin adsorbed to the particle surfaces, as a particle pellet forms after centrifugation. Using this information, the average recorded absorbance value for the supernatant prior to the first sample purification was 0.3708 ± 0.0005 absorbance units (AU, $n = 4$). Cross-referencing from the equation related to the empirically derived standard curve (ESM Fig. S1), this translates to a 0.373 ± 0.091 μg/mL streptavidin concentration remaining in the supernatant after centrifugation. Assuming that the change in concentration was significantly due to streptavidin adsorption on the hybrid surface microparticles, this corresponds to a $C_{min}$ of 0.627 ± 0.091 μg/mL. Using Eq. 3, the experimental results yield an 8.33 ± 1.21% which is within a standard deviation from the expected saturation coverage of 9.24 ± 1.47%. This confirms that streptavidin adsorbs to the particle surfaces after proper incubation and centrifugation is purifying the samples from unbound streptavidin.

## Fluorescence quantification for streptavidin adsorption

Once streptavidin adsorbs to the microparticle surface, biotin is used to form the functional linker between the particle and antibody. Similarly, to measure the streptavidin adsorption, a biotinylated fluorescence marker is utilized for optical characterizations. B4F is mixed with the sample and the fluorescence microscope captured images of the suspended particles, shown by Fig. 4. Figure 4a shows image under bright-field conditions to observe the particles in reference to the background solution. Following this, a green fluorescence protein (GFP) filter is applied and as expected, fluorescence intensities are highest at the Janus microparticle positions which represents the highest density of streptavidin in the image (Fig. 4b).

This is quantified by processing these images using the ImageJ software. Analytical image analysis is based on quantifying gray values of the pixels in the image. Image analysis show gray values (no units) for each pixel along a given line in an image ranging from 0 (black color) to 255 (white color). Figure 4c shows that pixel intensity from the microparticles is significantly greater than the background. We performed this analysis on ($n = 100$) microparticles over several images. The narrow variance of gray value intensity for the particles suggests that B4F and streptavidin attachment remains nearly uniform from particle to particle. The pixel values shown in image Fig. 4d correspond with the given pixel line measured from a slice of the fluorescent image. At this point, a trend of significantly increased gray value is seen for the pixels corresponding to the functionalized microparticles, with a 231.2 ± 18.4 average maximum gray value. This is greater than 3.5 times the gray value for the background intensity gray value of 64.7 ± 9.1.

Our analysis showed that streptavidin is not found in solution relative to adsorbed streptavidin on the hybrid surface particles. It also suggests that streptavidin molecule is not compromised through the adsorption process; this lends to the streptavidin tertiary structure having four binding sites with biotin placed on opposite protein surfaces. By ensuring if one side may be compromised from attachment with the particle, other regions remain active for biotin binding.

## Functionalization distribution on the hybrid microparticle

The uniform distribution of streptavidin on a particle should also be found to determine uniform streptavidin conjugation across the exposed polystyrene and $Al_2O_3$ surfaces. Equal spread across the entire particle surface area is important to ensure that all functionalized particles have the same probability for cell targeting regardless of contact point or angle. Figure 5 shows our MSI analytical approach to perform distribution analysis by quantifying gray value intensity for systematic orientations on the same particle. Here, maximum fluorescence intensity for a given particle is compared to relative intensities and intensity distributions at different retrieved angles from a top-down perspective of the particles (Fig. 5a). These angles include at 180° (1), 135° (2), 90° (3), and 45° (4). An unpaired $T$ test comparing maximum intensities recorded from the different orientations recorded no significant differences for any groups ($p > 0.05$ for all particle groups), and as a control, all intensities remained significantly larger than the background gray value ($p < 0.0001$ for all comparisons with the background intensities) as depicted by Fig. 5b. No significant differences from orientations enforce the protein adsorption kinetics of streptavidin to adhere to the polystyrene and $Al_2O_3$ surfaces with equal probability and coverage. In summary, our conjugation protocol detailed here required fewer steps and far fewer reagent volumes while retaining comparable adsorption efficiency and confirming equal distribution across a hybrid surface as compared to other studies. The comparative meta-analysis of our study is shown in ESM Table S2.

## Particle conjugation to human neutrophils

With the goal of cellular antigen classification, we validated the microparticle conjugation to human neutrophils. Deidentified human blood samples were obtained through

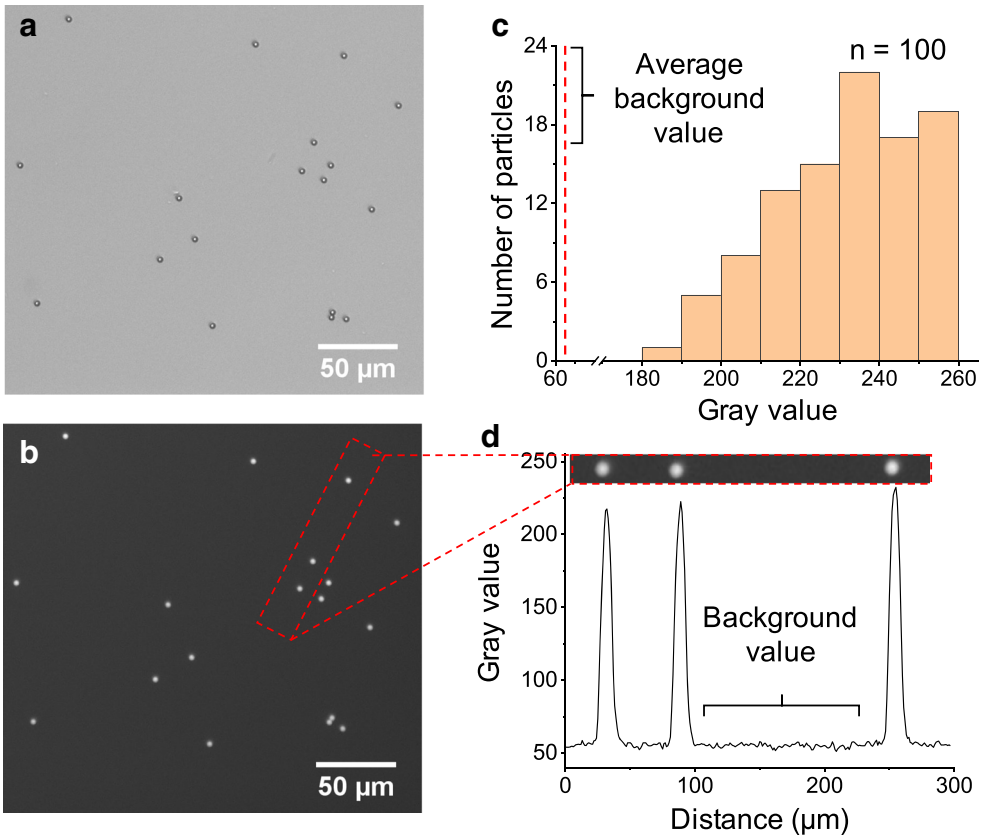


**Fig. 4** **a** Bright-field and **b** fluorescence imaging of microparticles functionalized with biotin-4-fluorescein dye. **c** Gray value quantification of fluorescence image using ImageJ. Fluorescence signals detected only along particle positions confirm biotin-streptavidin conjugation on microparticle surfaces. **d** Relative maximum fluorescence intensities measured through ImageJ for streptavidin-adsorbed Janus microparticles using biotin-4-fluorescein fluorescence markers ($n = 100$). Here, the fluorescence distribution on the particles is much greater than background intensity, signaling significantly larger streptavidin density on particles compared to soluble streptavidin. Scale bar = 50 μm for both images

an IRB study with Robert Wood Johnson Medical Hospital. Samples were collected from individuals with suspected sepsis conditions. CD11b differential regulation is considered a pro-inflammation biomarker for sepsis stratification [46].

Results showed neutrophil surface attachment with the functionalized microparticles (Fig. 6). Although all hybrid surface microparticles observed had streptavidin adsorption validated over 100 microparticles, Fig. 6 shows that all microparticles were not conjugated to the neutrophils. This may be due to the downregulation of CD11b antigen on neutrophils surface which is common under different inflammatory conditions of a patient. The differential regulation of CD11b antigen will be investigated in the future studies. For the sample presented, 30% of cells exhibited

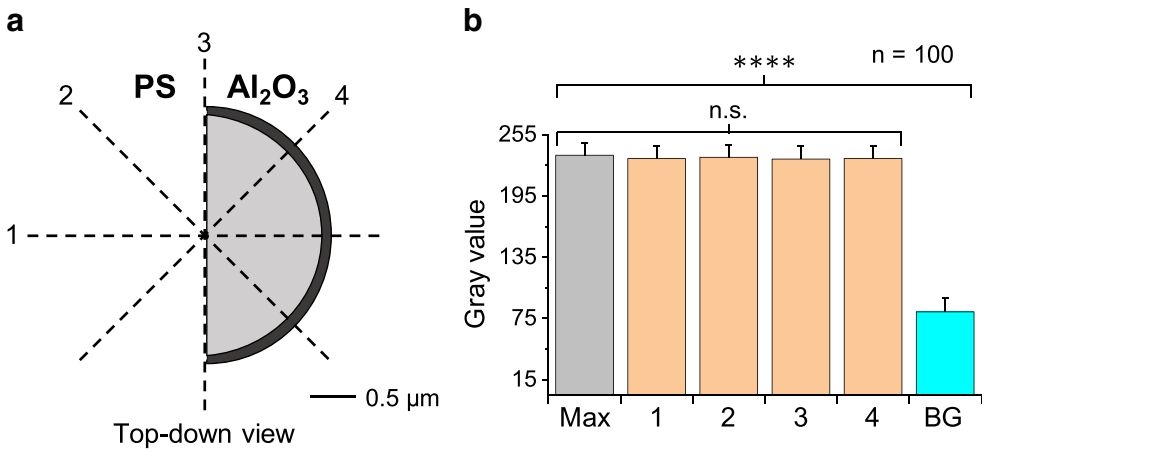


**Fig. 5** **a** Multi-sectional imaging approach of hybrid microparticles functionalized with biotin-4-fluorescein for fluorescence distribution analysis. Here, fluorescence intensity was measured at different orientations relative to the top surface of the particle to confirm equal distribution of streptavidin on polystyrene (white) and aluminum oxide (gray) surfaces (scale bar = 0.5 μm). **b** Average maximum intensity values from each orientation (yellow) relative to the maximum particle intensity (gray) as well as average background image (BG) gray value (cyan). Here, no significant (n.s.) differences between groups from an unpaired statistical *T* test ($n = 100$, $p > 0.05$) except for any comparison with the background group ($p < 0.0001$)

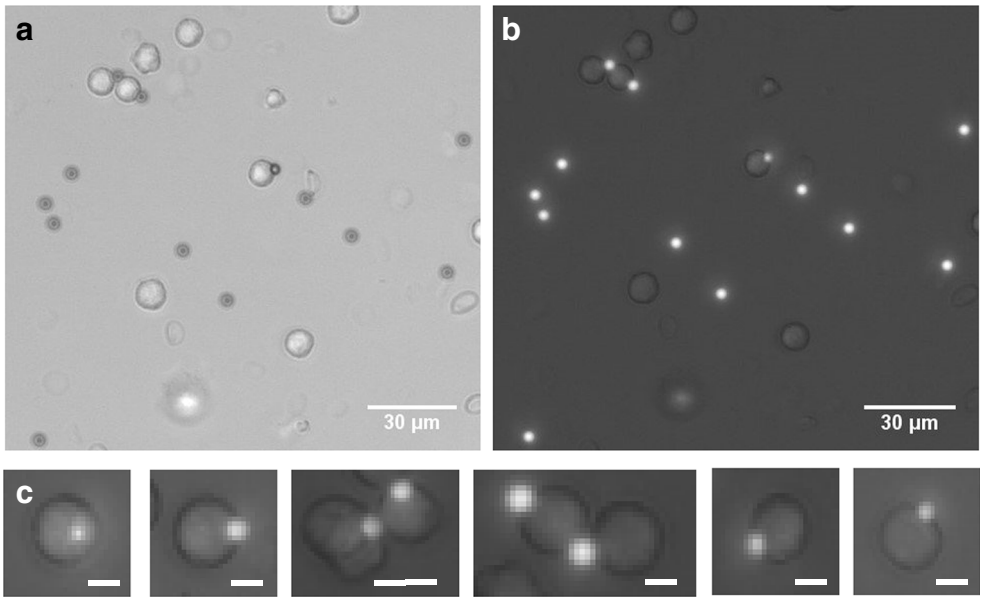


**Fig. 6** **a** Bright-field and **b** fluorescence imaging of functionalized Janus particles with isolated neutrophils. Here, biotin-4-fluorescein is used for improved Janus particle visualization, and neutrophils which express CD11b include functionalized particle attachment. **c** Isolated cases showcasing neutrophil-particle attachment under fluorescence imaging. Scale bars = 7 μm

functionalized particle attachment. Capitalizing on the multiple binding sites for streptavidin, B4F was added and used alongside biotinylated anti-CD11b antibodies to improve particle visualization under fluorescence microscopy (Fig. 6b). Here, functionalized particles are more distinctly identified in the sample, with cases for neutrophil-particle binding emphasized by Fig. 6c, showing single particles bound to one neutrophil, multiple particles bound to one neutrophil, and multiple neutrophils bound to one particle. Future studies will continue to evaluate particle attachment to neutrophils from sepsis-perceived samples and control those results to their serum lactate levels, which has also been attributed for sepsis diagnosis [47].

## Conclusion

This work demonstrates the functionalization of hybrid surface microparticles using simpler, quicker streptavidin-biotin multi-surface functionalization chemistry. Further, we provided an analytical model for implementing our optimized assay and developed a multi-sectional imaging (MSI) approach to validate the uniformity of functionalization on our hybrid surface microparticles. We validated our approach on polystyrene-$Al_2O_3$ hybrid microparticle and successfully conjugated anti-CD11b antibody on the microparticle. We further demonstrated the binding of antibody functionalized hybrid particles to the CD11b antigen on human neutrophils. The insulative properties from the metal oxide coatings fabricated into the hybrid surface particles entail they are measured uniquely under different voltage frequencies. From our previous reports, lab-on-a-chip impedance detection systems are sensitive enough to identify these polystyrene microparticles with a 10 nm difference in oxide layers as well as with different metal oxides, including titania, hafnia, and silica semi-coatings. Our goal with this functionalization technique is to use similar protocols for this library of microparticles with different targeting antibodies to evaluate antigen presence and deliver a novel multiplexing technology with a unipolar signal input and detection output. Building off the preliminary neutrophil-particle conjugation validation results, future studies will measure binding efficiencies over multiple controlled expression levels with hybrid surface particles of various metal oxides and functionalized targeting antibodies using this protocol, including those for disease-related cell receptors such as CD66b and neutrophil-expressed CD64. Such variation in binding of hybrid particles to antigen-presenting cells can be further exploited to quantify the antigen expression for disease pathogenesis in the future.

**Funding** We receive funding support from the Department of Electrical and Computer Engineering and Global Health Institute at Rutgers, The State University of New Jersey. We also receive support from NSF Award Number (2002511), Rutgers Vice Chancellor Research Innovation Grant. We also receive support from the Department of Education's Graduate Assistance in Areas of National Need (GAANN) program, P200A150131. Additionally, we receive support for this research from the National Institute of General Medical Sciences (NIGMS) as part of the National Institute of Health's (NIH) training grant T32 GM135141.

**Compliance with ethical standards** Blood samples were obtained from anonymous patients at Robert Wood Johnson Medical Hospital for whom a lactate test (a clinical test for suspicion of sepsis) is ordered by a physician. The left-over blood samples from patients after laboratory tests were deidentified by the clinical lab staff and sent to us. The study is approved by Rutgers The State University of New Jersey and Robert Wood Johnson Medical Hospital (Institutional Review Board (IRB) application # Pro2018002356).

**Conflict of interest** The authors declare that they have no conflicts of interest.

## References


1. Lee K, Yi Y, Yu Y. Remote control of T cell activation using magnetic Janus particles. Angew Chem Int Ed. 2016;55:7384–7.
2. Kadam R, Zilli M, Maas M, Rezwan K. Nanoscale Janus particles with dual protein functionalization. Part Part Syst Charact. 2018;35: 1700332.
3. Yang S, Guo F, Kiraly B, Mao X, Lu M, Leong KW, et al. Microfluidic synthesis of multifunctional Janus particles for biomedical applications. Lab Chip. 2012;12:2097–102.
4. Yi Y, Sanchez L, Gao Y, Yu Y. Janus particles for biological imaging and sensing. Analyst. 2016;141:3526–39.
5. Jung CW, Jalani G, Ko J, Choo J, Lim DW. Synthesis, characterization, and directional binding of anisotropic biohybrid microparticles for multiplexed biosensing. Macromol Rapid Commun. 2014;35: 56–65.
6. Liu Y, Dai R, Wei Q, Li W, Zhu G, Chi H, et al. Dual-functionalized Janus mesoporous silica nanoparticles with active targeting and charge reversal for synergistic tumor-targeting therapy. ACS Appl Mater Interfaces. 2019;11:44582–92.
7. Wang H, Li S, Zhang L, Chen X, Wang T, Zhang M, et al. Tunable fabrication of folic acid-Au@poly(acrylic acid)/mesoporous calcium phosphate Janus nanoparticles for CT imaging and active-targeted chemotherapy of cancer cells. Nanoscale. 2017;9:14322–6.
8. Sanchez L, Yi Y, Yu Y. Effect of partial PEGylation on particle uptake by macrophages. Nanoscale. 2017;9:288–97.
9. Zhang Q, Zhang L, Li S, Chen X, Zhang M, Wang T, et al. Designed synthesis of Au/Fe3O4@C Janus nanoparticles for dual-modal imaging and actively targeted chemo-photothermal synergistic therapy of cancer cells. Chem Eur J. 2017;23:17242–8.
10. Springer TA. Traffic signals for lymphocyte recirculation and leukocyte emigration: the multistep paradigm. Cell. 1994;76:301–14.
11. Biron BM, Ayala A, Lomas-Neira JL. Biomarkers for sepsis: what is and what might be? Biomark Insights. 2015;10s4:BMI.S29519.
12. Hassan U, Ghonge T, Reddy B Jr, Patel M, Rappleye M, Taneja I, et al. A point-of-care microfluidic biochip for quantification of CD64 expression from whole blood for sepsis stratification. Nat Commun. 2017;8:1–12.
13. Watkins NN, Hassan U, Damhorst G, Ni H, Vaid A, Rodriguez W, et al. Microfluidic CD4+ and CD8+ T lymphocyte counters for point-of-care HIV diagnostics using whole blood. Sci Transl Med. 2013;5:214ra170.
14. Tanino M, Matoba R, Nakamura S, Kameda H, Amano K, Okayama T, et al. Prediction of efficacy of anti-TNF biologic agent, infliximab, for rheumatoid arthritis patients using a comprehensive transcriptome analysis of white blood cells. Biochem Biophys Res Commun. 2009;387:261–5.
15. Hodgson LE, Venn RM, Short S, Roderick PJ, Hargreaves D, Selby N, et al. Improving clinical prediction rules in acute kidney injury with the use of biomarkers of cell cycle arrest: a pilot study. Biomarkers. 2019;24:23–8.
16. Mukhopadhyay S, Taylor JA, Kohorn IV, Flaherman V, Burgos AE, Phillipi CA, et al. Variation in sepsis evaluation across a national network of nurseries.Pediatrics. 2017;139:e20162845. https://doi.org/10.1542/peds.2016-2845. Accessed 19 Nov 2019.
17. Reddy B, Hassan U, Seymour C, Angus DC, Isbell TS, White K, et al. Point-of-care sensors for the management of sepsis. Nat Biomed Eng. 2018;2:640–8.
18. Hein-Kristensen L, Wiese L, Kurtzhals JAL, Staalsoe T. In-depth validation of acridine orange staining for flow cytometric parasite and reticulocyte enumeration in an experimental model using Plasmodium berghei. Exp Parasitol. 2009;123:152–7.
19. Venet F, Lepape A, Monneret G. Clinical review: flow cytometry perspectives in the ICU - from diagnosis of infection to monitoring of injury-induced immune dysfunctions. Crit Care. 2011;15:231.
20. Umlauf VN, Dreschers S, Orlikowsky TW. Flow cytometry in the detection of neonatal sepsis. Int J Pediatr. 2013;2013:763191. https://doi.org/10.1155/2013/763191. Accessed 14 May 2020.
21. Xie P, Cao X, Lin Z, Javanmard M. Top-down fabrication meets bottom-up synthesis for nanoelectronic barcoding of microparticles. Lab Chip. 2017;17:1939–47.
22. Ahuja K, Rather GM, Lin Z, Sui J, Xie P, Le T, et al. Toward point-of-care assessment of patient response: a portable tool for rapidly assessing cancer drug efficacy using multifrequency impedance cytometry and supervised machine learning. Microsyst Nanoeng. 2019;5:1–11.
23. Hassan U, Bashir R. Electrical cell counting process characterization in a microfluidic impedance cytometer. Biomed Microdevices. 2014;16:697–704.
24. Chen J, Xue C, Zhao Y, Chen D, Wu M-H, Wang J. Microfluidic impedance flow cytometry enabling high-throughput single-cell electrical property characterization. IJMS. 2015;16:9804–30.
25. Sheneef A, Mohamed T, Boraey NF, Mohammed MA. Neutrophil CD11b, CD64 and lipocalin-2: early diagnostic markers of neonatal sepsis. Egypt J Immunol. 2017;24:29–36.
26. Khan SQ, Khan I, Gupta V. CD11b activity modulates pathogenesis of lupus nephritis. Front Med. 2018:5;52. https://doi.org/10.3389/fmed.2018.00052. Accessed 23 May 2020.
27. Monopoli MP, Walczyk D, Campbell A, Elia G, Lynch I, Baldelli Bombelli F, et al. Physical−chemical aspects of protein corona: relevance to in vitro and in vivo biological impacts of nanoparticles. J Am Chem Soc. 2011;133:2525–34.
28. Vilanova O, Mittag JJ, Kelly PM, Milani S, Dawson KA, Rädler JO, et al. Understanding the kinetics of protein–nanoparticle corona formation. ACS Nano. 2016;10:10842–50.
29. Calais T, Bourrier D, Bancaud A, Chabal Y, Estève A, Rossi C. DNA grafting and arrangement on oxide surfaces for self-assembly of Al and CuO nanoparticles. Langmuir. 2017;33:12193–203.
30. Välimaa L, Pettersson K, Rosenberg J, Karp M, Lövgren T. Quantification of streptavidin adsorption in microtitration wells. Anal Biochem. 2004;331:376–84.
31. Jain A, Cheng K. The principles and applications of avidin-based nanoparticles in drug delivery and diagnosis. J Control Release. 2017;245:27–40.
32. Goebel-Stengel M, Stengel A, Taché Y, Reeve JR. The importance of using the optimal plastic and glassware in studies involving peptides. Anal Biochem. 2011;414:38–46.
33. Castelino K, Kannan B, Majumdar A. Characterization of grafting density and binding efficiency of DNA and proteins on gold surfaces. Langmuir. 2005;21:1956–61.
34. Dolci M, Bryche J-F, Leuvrey C, Zafeiratos S, Gree S, Begin-Colin S, et al. Robust clicked assembly based on iron oxide nanoparticles for a new type of SPR biosensor. J Mater Chem C. 2018;6:9102–10.
35. Klumb LA, Chu V, Stayton PS. Energetic roles of hydrogen bonds at the ureido oxygen binding pocket in the streptavidin−biotin complex. Biochemistry. 1998;37:7657–63.
36. Weber PC, Ohlendorf DH, Wendoloski JJ, Salemme FR. Structural origins of high-affinity biotin binding to streptavidin. Science. 1989;243:85–8.
37. Ylikotila J, Välimaa L, Takalo H, Pettersson K. Improved surface stability and biotin binding properties of streptavidin coating on polystyrene. Colloids Surf B Biointerfaces. 2009;70:271–7.
38. Li S, Liu H, He N. Covalent binding of streptavidin on gold magnetic nanoparticles for bead array fabrication. J Nanosci Nanotechnol. 2010;10:4875–82.

39. Oohora K, Burazerovic S, Onoda A, Wilson YM, Ward TR, Hayashi T. Chemically programmed supramolecular assembly of hemoprotein and streptavidin with alternating alignment. Angew Chem. 2012;124:3884–7.
40. Johnson M. Protein quantitation. Mater Methods. 2012;2:15. https://doi.org/10.13070/mm.en.2.115.
41. Contado C, Mehn D, Gilliland D, Calzolai L. Characterization methods for studying protein adsorption on nano-polystyrene beads. J Chromatogr A. 2019;1606:460383.
42. Quevedo PD, Behnke T, Resch-Genger U. Streptavidin conjugation and quantification—a method evaluation for nanoparticles. Anal Bioanal Chem. 2016;408:4133–49.
43. Lynch I, Dawson KA. Protein-nanoparticle interactions. Nano Today. 2008;3:40–7.
44. Nakanishi K, Sakiyama T, Kumada Y, Imamura K, Imanaka H. Recent advances in controlled immobilization of proteins onto the surface of the solid substrate and its possible application to proteomics. Curr Proteom. 2008;5:161–75.
45. Williams EH, Davydov AV, Motayed A, Sundaresan SG, Bocchini P, Richter LJ, et al. Immobilization of streptavidin on 4H–SiC for biosensor development. Appl Surf Sci. 2012;258:6056–63.
46. Sharma A, Thakur A, Bhardwaj C, Kler N, Garg P, Singh M, et al. Potential biomarkers for diagnosing neonatal sepsis. Curr Med Res Pract. 2020:10;12-7. https://doi.org/10.1016/j.cmrp.2019.12.004. Accessed 20 Jan 2020.
47. Lee SM, An WS. New clinical criteria for septic shock: serum lactate level as new emerging vital sign. J Thorac Dis. 2016;8:1388–90.